(Preprint) AAS 21-721

EVALUATION OF LOW-THRUST SYNERGETIC MANEUVERS DURING PLANETARY FLYBYS

Ghanghoon Paik*, Robert G. Melton†

Previous interplanetary missions have used non-powered flyby maneuvers to gain delta-v via gravity assist. In this research, trajectories similar to previous missions are studied to compare the effect of applied continuous thrust while a spacecraft is flying inside a planet's sphere of influence. Compared to a free flyby, a spacecraft with continuous thrust capability can optimize the path and possibly allow a wider window for mission design. The focus is a proof-of-concept for gravity assists using continuous thrust within the SOI of each encountered planet for a synergetic Δv. With further development, it is expected to generate optimized trajectories to target a planet with powered gravity assist. In the interplanetary results, the algorithm was able to find a path with two successful powered planetary flybys from a given set of dates.

INTRODUCTION

Multiple gravity assist maneuvers are one of the techniques applied on deep space missions including the Cassini, Galileo, and Voyager missions. The gravity assist allows a spacecraft to change its velocity without burning propellant; instead, the spacecraft exchanges momentum with the body that it flies by. Since the major benefit comes from a free Δv, it is also possible to apply thrust during the maneuver in order to boost the influence (i.e., a low-thrust synergetic maneuver). With the application of boost, efficiency of the propulsive maneuver can be largely improved, which is called the Oberth effect.[1] There are two possible options for the propulsive maneuver in order to achieve the maximum output from the maneuver depending on the frame of reference. The trajectory of a gravity assist maneuver can have two different characteristics, elliptical and hyperbolic paths.[2,3] The elliptical path occurs outside of the planet's sphere of influence (SOI) and the hyperbolic path occurs inside the planet's SOI. Impulsive thrust would be applied at the periapsis of each orbit to maximize the benefit. Both cases are visually represented in Figure 1.

Research previously done on applied thrust with gravity assist has been mainly focused on either periapsis of elliptical paths or deep space maneuvers (DSMs) to target the next planetary encounter.[4–11] The former approach is used to gain extra Δv by using the Oberth effect either via impulsive or continuous thrust, and the latter one is using multiple burns to generate a feasible trajectory between two planets.

In this research, the conceptually similar approach to an elliptical path with a thrust is used to apply the Oberth effect as shown in Figure 1a. For the interplanetary mission, an elliptical path occurs when a spacecraft flies around the Sun and a hyperbolic path occurs when the spacecraft is

*PhD candidate, Department of Aerospace Engineering, Pennsylvania State University, University Park, PA 16802
†Professor, AAS Fellow, AIAA Associate Fellow, Department of Aerospace Engineering, Pennsylvania State University, University Park, PA 16802

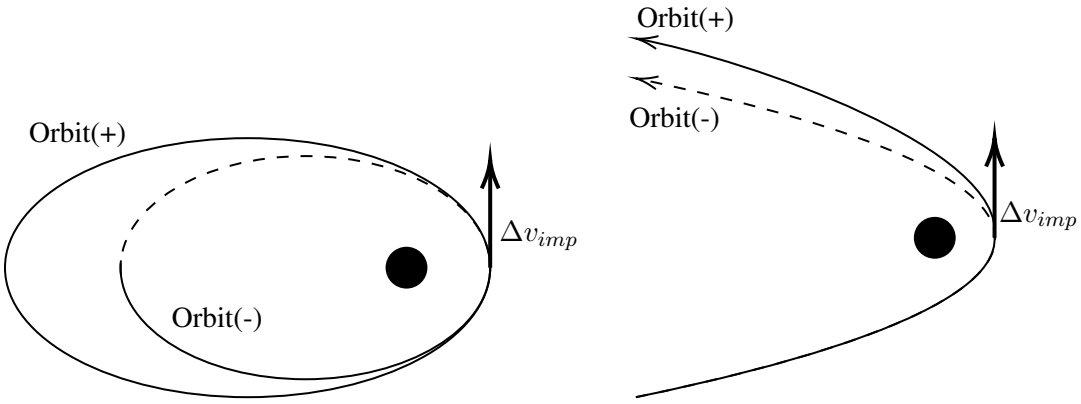

(a) Elliptical trajectory case (b) Hyperbolic trajectory case

Figure 1: Oberth effect with impulsive Δv

traveling inside a planet's SOI. In terms of time scale, the spacecraft stays within a planet's SOI a significantly shorter amount of time compared to a heliocentric orbit. Thus, applying a continuous thrust during the planetary fly could be simplified to an impulsive maneuver in the heliocentric frame. Therefore, the technique introduced in this paper is developed to apply a continuous thrust to simulate a synergetic maneuver and study the possibilities and potentials of the method.

METHODS

In the work, in order to generate a multiple gravity assist trajectory, methods including spacecraft dynamics, differential evolution, targeting for planetary encounters, and the powered flyby are applied.

The spacecraft has the capability to perform continuous thrust of up to $10N$ which can be pointed toward any direction. The movement of the spacecraft is 2 dimensional for simplicity, and polar form of two-body problem is used to describe the motion. A differential evolution algorithm is applied to find optimal direction and magnitude of the thrust.

Spacecraft Dynamics

Assuming planar motion only for the spacecraft (and projecting the planet's positions onto the J2000 ecliptic plane), the equations of motion are represented in polar coordinate form as

$$\dot{\vec{x}} = \begin{bmatrix} v_r \\ -\frac{\mu - r\ v_\theta^2}{r^2} \\ \frac{v_\theta}{r} \\ -\frac{v_r\ v_\theta}{r} \end{bmatrix} \tag{1}$$

where $\vec{x} = [r,\ v_r,\ \theta,\ v_\theta]^T$, with components of radial distance, radial velocity, angular displacement from x-axis, and transverse velocity, respectively.[12–15] In order to include finite thrust in the

dynamics, an extra term is introduced

$$\dot{\vec{x}} = \begin{bmatrix} v_r \\ -\frac{\mu - r\, v_\theta^2}{r^2} \\ \frac{v_\theta}{r} \\ -\frac{v_r\, v_\theta}{r} \end{bmatrix} + \frac{T}{m} \begin{bmatrix} 0 \\ \sin\beta \\ 0 \\ \cos\beta \end{bmatrix}. \tag{2}$$

In Eq. (2), T/m is the thrust-to-mass ratio and β is the thrust-pointing angle which is determined by the third-order polynomial

$$\beta = \beta_1 + \beta_2 t + \beta_3 t^2 + \beta_4 t^3. \tag{3}$$

The thrust pointing angle, β, is relative to the local horizontal plane.

Differential Evolution Algorithm

Differential evolution (DE) is an heuristic technique to find an optimal solution through iterative update of candidate solutions.[16,17] The result of DE largely depends on three main parameters, F, C_r, and N_p which are scale factor, crossover rate, and population size, respectively. Each member of the population (i.e. each potential solution) contains n components (i.e. decision variables). In general, values of parameters are selected from the range in $F \in [0, 2]$ and $C_r \in [0, 1]$. Each parameter value is problem specific and need to be adjusted accordingly to achieve the optimal solution. Starting with randomly generated initial solutions, during each iteration, compare position of current and previous step and update the position if the current one shows improvement. The process repeats until certain criteria are met including maximum number of iterations or convergence reached. In this research, a few modifications were made to the basic algorithm, with the result described in Algorithm 1. Compared to the basic algorithm which uses three design points, five design points are selected to generate potential new positions. This selection model is called best-2 and it shows a better performance and higher accuracy than other schemes tested. Previously, instead of differential evolution, particle swarm optimization (PSO) was applied to solve the problem. PSO was also a highly effective heuristic approach which can provide accurate enough solutions. However, PSO had a tendency to fall into local minima quite often while DE rarely has such issue in this application. When it gets trapped in a wrong solution, the algorithm often never converges which is a significant problem when the process is automated. Also, in terms of computation time, DE shows better performance. In order to let the program run automatically over a given large time window without falling into local minima, DE is selected.

Differential evolution algorithm is used to find optimal thrust pointing angle and magnitude for each continuous thrust maneuver. Each member of the population has 10 components

$$P = [\beta_1, \beta_2, \beta_3, \beta_4, N_{thr,1}, \beta_1', \beta_2', \beta_3', \beta_4', N_{thr,2}] \tag{4}$$

where β_i and β_i' are polynomial coefficients for thrust pointing angle from Eq. (3) and the $N_{thr,i}$ are magnitudes of thrust. The first five values are used to represent thrust characteristics before reaching periapsis and the rest are after periapsis passage inside a planet's SOI.

The cost function to be minimized is represented by a sum of three penality terms

$$J = -|\Delta v_f| + \alpha|\Delta r_p| + \gamma \tag{5}$$

Algorithm 1: Modified version of differential evolution algorithm

randomly generate initial population of size N_p;
choose F and C_r values;
while *solution is not converged or iteration* $k \leq 500$ **do**
  for *each member* j *in the population* **do**
    generate 5 distinct design points, $r_1, r_2, ..., r_5 \in (1, N_p)$ where $r_1 \neq r_2, ..., \neq r_5$;
    generate random integer $j_r \in (1, n)$;
    if $j = j_r$ *or* $rand(0,1) < C_r$ **then**
      $U_j^k = x_{(j,r_1)}^k + F(x_{(j,r_2)}^k - x_{(j,r_3)}^k) + F(x_{(j,r_4)}^k - x_{(j,r_5)}^k)$;
    else
      $U_j^k = x_j^k$;
    end
    if $f(\mathbf{U}^k) \leq f(\mathbf{x}^k)$ **then**
      $\mathbf{x}^{k+1} = \mathbf{U}^k$
    else
      $\mathbf{x}^{k+1} = \mathbf{x}^k$
    end
  end
end

where $|\Delta v_f|$ is the difference in final velocity with and without continuous thrust after flyby, Δr_p is the difference in periapsis altitude with and without the thrust and γ penalizes the cost function if next planetary encounter is not found,

$$\gamma = \begin{cases} 15 & \text{if no encounter was found} \\ 10 & \text{if encounter was found but unable to flyby} \\ 0 & \text{if encounter was found and can perform flyby.} \end{cases} \tag{6}$$

For the clarification of each condition, encounter indicates the spacecraft approaches approximately $1.5\, r_{SOI}$ or less away from the planet. Then, flyby-ability is determined by the spacecraft's orbital characteristics. The spacecraft is deemed "unable to flyby" if its speed is much faster than a planet, or it enters and leaves the SOI without having a chance to interact with the flyby planet. Therefore, the cost function will be penalized based on the condition that is met. The factor α is an inequality constraint weight that is defined as

$$\alpha = \begin{cases} 0 & \text{if } |\Delta r_p| < 10^{-3} \\ 1000 & \text{if } |\Delta r_p| > 10^{-3} \end{cases} . \tag{7}$$

The penalty terms help to drive the optimization process toward a feasible solution.

Planetary Encounter Targeting

At this stage, a sophisticated method to accurately plan planetary encounters is not fully developed. In order to find a sequence for multiple flyby's, an exhaustive search to find the optimal launch/arrival window was done within a month of the launch window ($\pm$ 30 days) with increment

of a day for an actual mission. In this research, searched launch and arrival dates refer to the launch date from Earth and the arrival date to a first-encounter planet. However, various options are considered to schedule the multiple gravity assist mission. The Δv isoline plot can be used to estimate the baseline time frame for the mission. From the estimation, the possibility of generating a feasible trajectory can be identified within a given launch window. Since each planet has to be accessible by the spacecraft at the time of arrival, determining positions of both the spacecraft and planets is required. Several different methods including search algorithms and cluster analysis are considered to be applied for trajectory scheduling and planetary targeting.

For the moment, added penalty that checks the next planetary encounter allows the DE optimizer to find the possible path to the next planet. Testing for the next encounter is done by the algorithm that compares the spacecraft's trajectory and each planet's orbital position. Each time the spacecraft crosses the planet's orbit, algorithm checks whether the planet is within a certain distance away or not for the spacecraft to get inserted into the planet's SOI. As described in Eq. (6), the amount of penalty varies depending on the condition.

The steps to apply the described methods are shown in the flow chart in Figure 2. An initial launch/arrival window is given to the program, it looks for the best entry point to the SOI. Then, differential evolution searches for the next possible encounter. If the encounter is found, the Keplerian trajectory to the next planet is generated and the DE process repeats until the spacecraft arrives at the target planet. If DE fails to find the next encounter, the search moves on to a different set of dates.

RESULTS

In this work, several assumptions are made, including the specification of a spacecraft and the minimum approach distance to a planet. The mass of the spacecraft is assumed to be 2000 kg, the exhaust velocity of the thrusters is 50 km/s, and the maximum thrust magnitude is 10 N. Then, mass flow rate for the powered maneuver can be calculated from

$$\dot{m} = \frac{T}{v_e} \tag{8}$$

where v_e is the exhaust velocity of the thruster and T is thrust magnitude. At its maximum thrust of 10 N, $\dot{m}$ is 0.72 kg/hr or 17.28 kg/day. At constant thrust, the thrust-to-mass ratio (T/m) at any given time, t, can be represented as

$$\begin{aligned} \frac{T}{m(t)} &= \frac{T}{m_0 - \dot{m}\, t} \\ &= \frac{T}{m_0 - T/v_e\, t} \end{aligned} \tag{9}$$

for the initial mass of the spacecraft, m_0. The required power for the spacecraft is not considered in this work and assumed to be available throughout the duration of the entire mission. Thrust magnitudes and pointing vectors are independently evaluated for before and after the periapsis passage. Also, the safetapproach distance to the planet is assumed to be 5 percent of the planet's radius. Thus, the spacecraft must fly a certain altitude above the surface to avoid influence of a planet's atmosphere.

However, more massive planets have larger SOI radii and require the spacecraft to thrust for longer durations. For example, flyby within Jupiter's SOI may take over 60 days to complete and

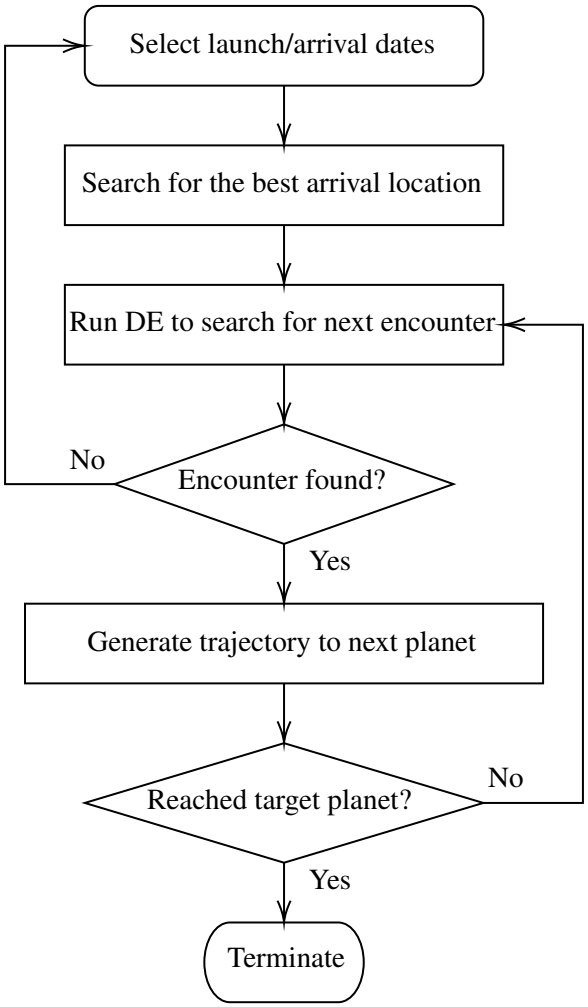

Figure 2: Flow chart of main steps to generate mission trajectory

can burn more than 1000 kg of propellant at the maximum thrust level. In order to avoid depletion of propellant onboard, thrusters are considered to be turned on only when $r \leq 0.6\, r_{SOI}$.

In this paper, the initial stage of a Voyager-like mission is demonstrated. Figure 4 shows comparison between free and powered flyby inside Jupiter's SOI. The entry and departure angles are measured from the x-axis which is inertially fixed. Since the ecliptic coordinate at J2000 is used, the x-axis on both the planetocentric and heliocentric coordinates points toward the vernal equinox of the Sun. The visual representation of the coordinate system is found in Figure 3.

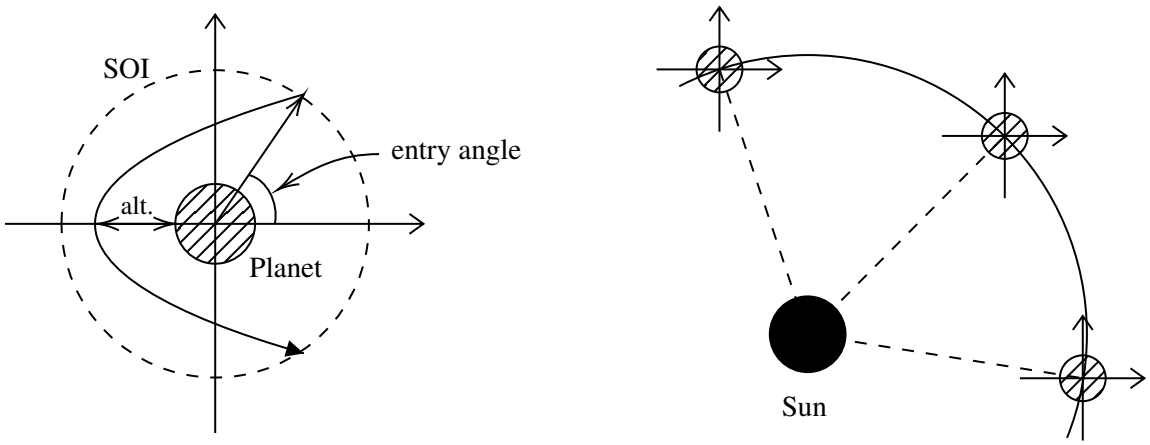

Figure 3: Visual description of terms and coordinate system

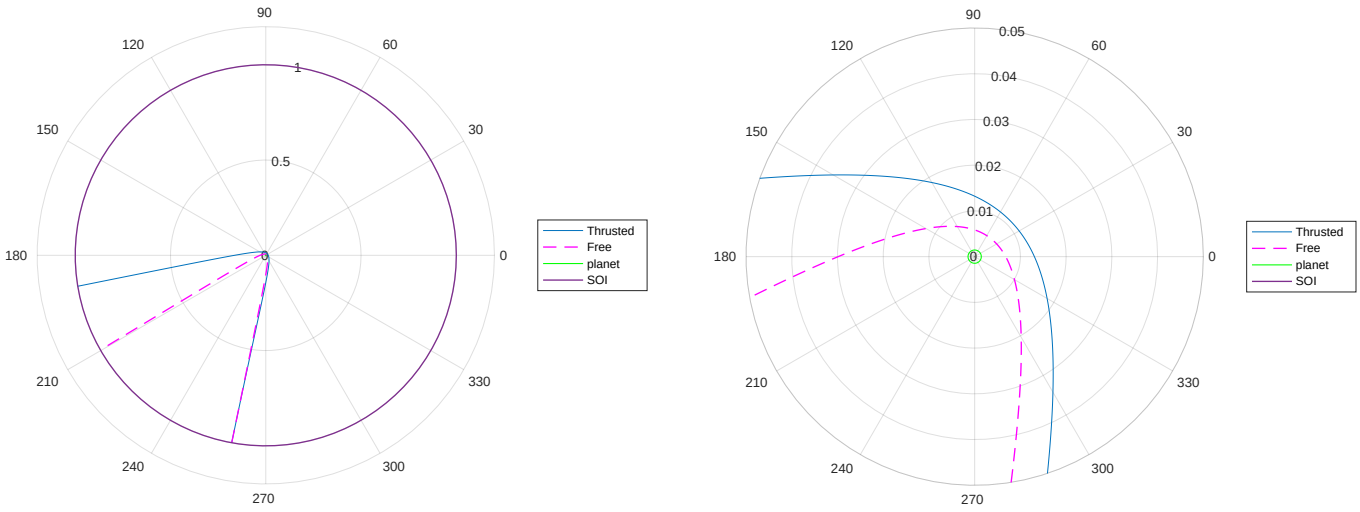

(a) Free vs. thrusted trajectory inside the SOI

(b) Free vs. thrusted trajectory near the planet

Figure 4: Comparison of resulting trajectories with and without continuous thrust of Jupiter flyby

Figure 4 shows trajectories of both free and powered flyby's around Jupiter. Both trajectories describes tight turns around the planet. However, the thrusted version has a higher periapsis altitude which may indicate a Δv loss. The spacecraft enters Jupiter's SOI at approximately the 260 degree

location and departs at 210 degrees (free flyby) or 190 degrees (powered flyby). For the Jupiter encounter, the spacecraft flies in front of the planet and loses some velocity in order to make the next encounter with Saturn.

Figure 5 is showing the difference between free and powered flyby inside Saturn's SOI. In this case, the spacecraft is flying almost a straight line passing Saturn slightly over $0.05\,r_{SOI}$ when thrust is turned off. On the other hand, with the continuous thrust, the spacecraft flies approximately 35650 km ($0.00065\,r_{SOI}$) above the surface and with 101.7 degree turn angle. After the Saturn flyby, the heliocentric trajectory is dramatically turned. However, a Uranus or Neptune encounter is not found with the given orbital characteristics.

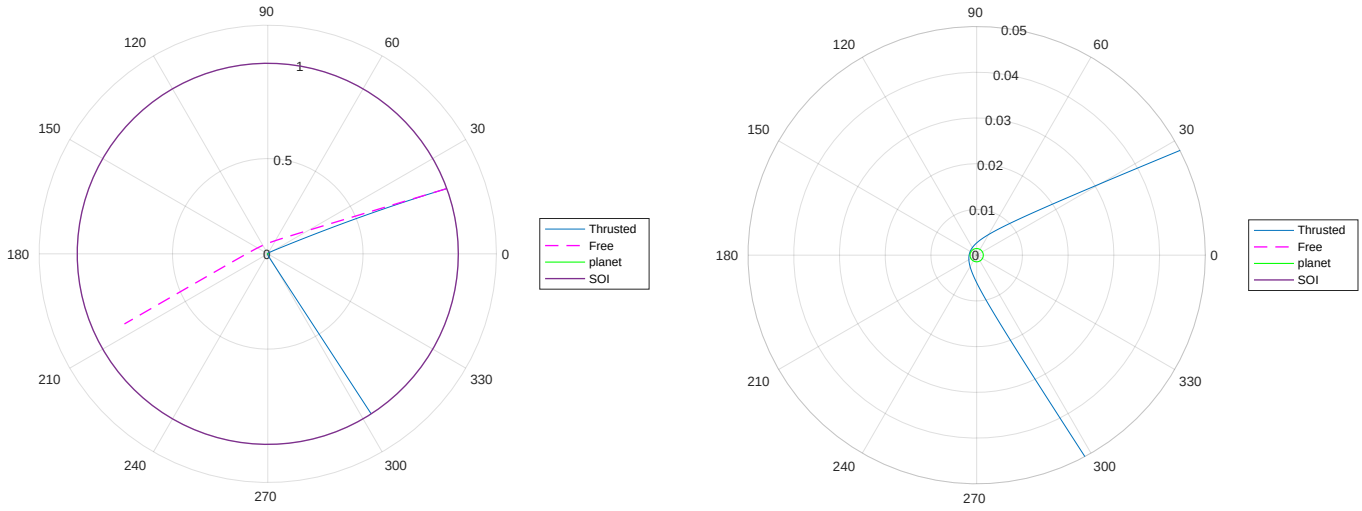

(a) Free vs. thrusted trajectory inside the SOI

(b) Free vs. thrusted trajectory near the planet

Figure 5: Comparison of resulting trajectories with and without continuous thrust of Saturn flyby

Figures 6 and 7 show thrust pointing angle and magnitude of the thrust during Jupiter and Saturn flybys. The left and right half of each plot represent thrust characteristics of incoming and outgoing trajectory while red star indicates TOF of periapsis passage. The constant-thrust trajectory is plotted with a straight dashed-line. The thrust pointing angle is measured from the local horizontal plane. The heliocentric trajectory of the spacecraft is represented in Figure 8. After departing from Jupiter around August 6, 1979, the spacecraft approaches close to Saturn on July 3, 1981. The data from those synergetic maneuvers are given in Table 1.

The generated trajectory in Figure 8 failed to visit Uranus or Neptune even though it has a similar Saturn turn compared with the Voyager 2 mission. Since the planetary encounter requires precise scheduling and targeting, it is not surprising to miss one or both encounters. While Voyager 1 and 2 were launched around September 5, 1977 and August 20, 1977, respectively, this simulation uses Earth launch date of June 15, 1977 which is few months ahead of both Voyager missions. Also, this simulation uses continuous thrust during the flyby inside the SOIs which can alter the characteristics even when the same dates are used.

Since the simulation is modeling the Voyager 2 mission, all four planetary flybys (Jupiter, Saturn, Uranus, and Neptune) are initially expected. However, the goal for this technique is not to recreate

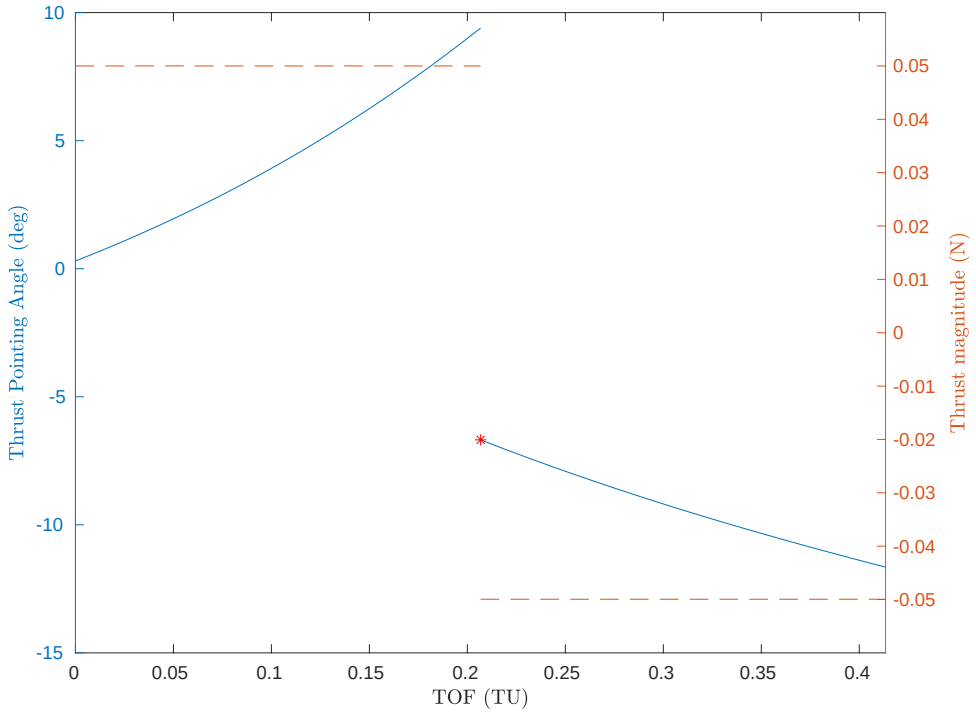

Figure 6: Thrust pointing angle and magnitude during the first powered Jupiter flyby

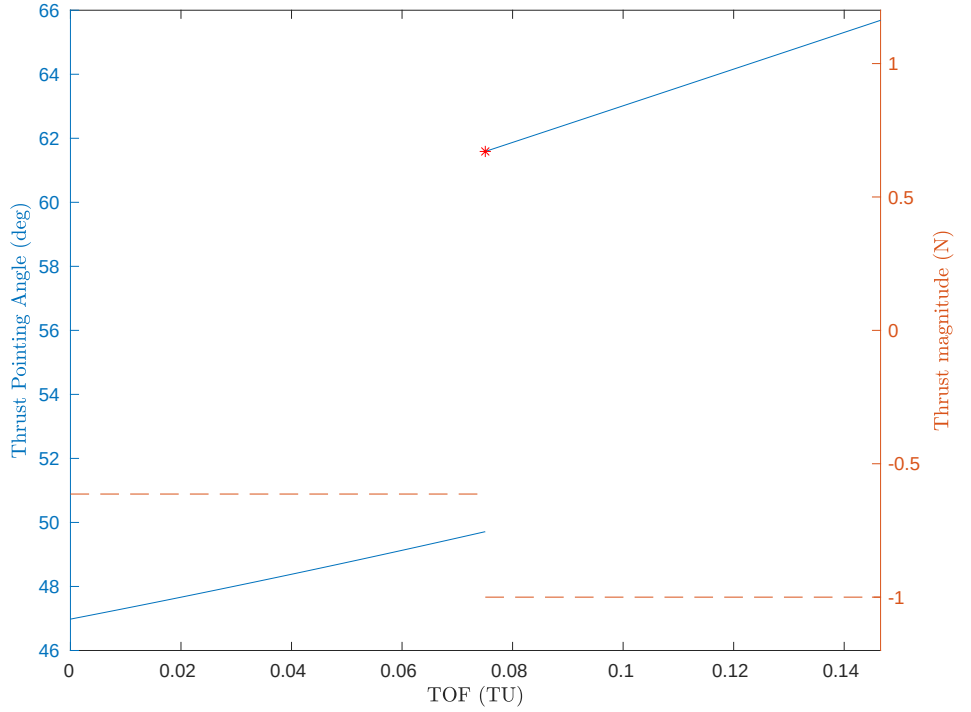

Figure 7: Thrust pointing angle and magnitude during the first powered Saturn flyby

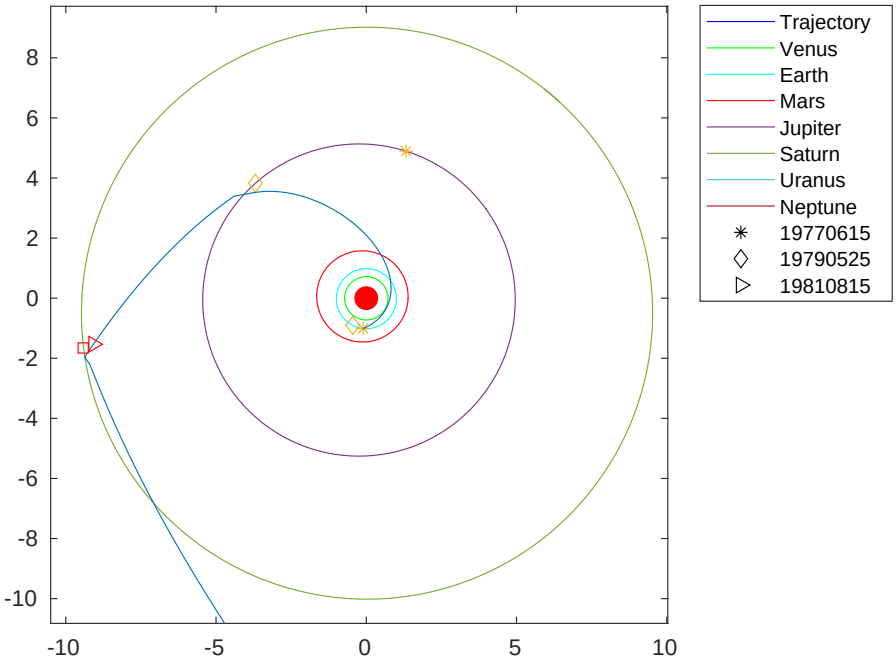

Figure 8: Voyager-like trajectory with gravity assist

	Jupiter	Saturn
Arrival	1979-05-25	1981-07-03
Departure	1979-08-06	1981-08-15
Δv (km/s)	-11.9	17.3
Thrust$_{in}$ (N)	0.05	-0.57
Thrust$_{out}$ (N)	-0.05	-1
$r_{p,alt}$ (km)	462780.2	35649.8
Δm (kg)	15.3	139.2
Turn angle (deg)	109.6	101.8

Table 1: Data from Jupiter and Saturn flybys

the previous missions but to offer a different perspective or approach for designing multiple gravity assist mission. From this point of view, though it is not completely satisfied, it shows enough potential for further development and presents room to be improved.

CONCLUSION

In this work, continuous thrust is applied inside of planet's SOIs during flybys to generate a synergetic gravity assist trajectory. At this stage of development, the technique is using the exhaustive search method from given launch and arrival dates to find the optimal set of dates. For example, Voyager 2 mission dates are provided to the algorithm as a reference date. Due to the nature of the exhaustive method, it requires a significant amount of compute power and time.

The results shows a Voyager-type trajectory with Jupiter and Saturn encounters. Even though the trajectory has a pattern after Saturn flyby similar to that of Voyager 2, Uranus or Neptune encounters are not found. This version of the method optimizes only the current stage of the trajectory instead of considering next steps. This issue could be improved by combining a backward search from the final target toward the Earth. Once both trajectories are generated, their results could be collectively used to finalize the optimal path. Although the technique is still under development, the current version of the method is able to show the potential to find a trajectory that can visit multiple planets if the mission is properly scheduled.

After testing against other previous missions or simulation data, it is expected to automatically generate a multiple gravity assist mission trajectory with synergetic maneuvers. With the development of a better scheduling algorithm, the computational efficiency could be improved over the pure exhaustive approach. Currently, it is unable to guess a spacecraft launch date for multiple planetary encounters without having a good initial guess, which is the reason why the Voyager 2 mission launch date is used as an initial guess. In the future, an algorithm to predict potential dates for multiple gravity assist mission can be developed along with the introduced technique to automatically generate a fully distinct mission plan. Potentially, use of search algorithms, i.e. dynamic programming, traveling salesman problem algorithm, or graph search methods, could be considered to generate with starting points for the mission planning.

Whereas this paper considers only outer-planet encounters, simulations for inner planets and combinations of inner/outer planets model are also being considered and actively investigated. Future work will examine these complex cases in the search for more mission opportunities.

NOTATION

J	cost function
m	spacecraft mass
$\dot{m}$	mass flow rate
N_{thr}	thrust thrust magnitude
r	radial distance
r_p	radius of periapsis
T	thrust magnitude
t	time
v_r	radial velocity
v_θ	transverse velocity
$\vec{x}$	state vector
α	penalty multiplier
β	thrust pointing angle
β_i	polynomial coefficients of thrust pointing angle ($i = 1, ..., 4$)
Δv	change in velocity before and after the maneuver
Δv_{imp}	change in velocity by impulsive maneuver
Δr_p	difference in periapsis distance
Δv_f	difference in final velocity (with and without thrust)
δ	turn angle
γ	planetary encounter penalty
θ	angular displacement from x-axis
μ	standard gravitational parameter

REFERENCES

[1] H. Oberth, "Ways to spaceflight," techreport, NASA Techdocs, 1972.

[2] A. F. S. Ferreira, A. F. B. A. Prado, and O. C. Winter, "A numerical mapping of energy gains in a powered Swing-By maneuver," *Nonlinear Dynamics*, Vol. 89, No. 2, 2017, pp. 791–818, https://doi.org/10.1007/s1107.

[3] A. F. B. d. Almeida Prado and G. d. Felipe, "An analytical study of the powered swing-by to perform orbital maneuvers," *Advances in Space Research*, Vol. 40, No. 1, 2007, pp. 102–112, https://doi.org/10.1016/j.asr.2007.04.09.

[4] M. Ceriotti and M. Vasile, "MGA trajectory planning with an ACO-inspired algorithm," *Acta Astronautica*, Vol. 67, No. 9-10, 2010, pp. 1202–1217.

[5] J. Englander, B. Conway, and T. Williams, "Automated Interplanetary Trajectory Planning," *AIAA/AAS Astrodynamics Specialist Conference*, 2012.

[6] D. H. Ellison, B. A. Conway, J. A. Englander, and M. T. Ozimek, "Analytic Gradient Computation for Bounded-Impulse Trajectory Models Using Two-Sided Shooting," *Journal of Guidance, Control, and Dynamics*, Vol. 41, No. 7, 2018, pp. 1449–1462, 10.2514/1.G003077.

[7] D. H. Ellison, B. A. Conway, J. A. Englander, and M. T. Ozimek, "Application and Analysis of Bounded-Impulse Trajectory Models with Analytic Gradients," *Journal of Guidance, Control, and Dynamics*, Vol. 41, No. 8, 2018, pp. 1700–1714, 10.2514/1.G003078.

[8] A. Gad and O. Abdelkhalik, "Hidden Genes Genetic Algorithm for Multi-Gravity-Assist Trajectories Optimization," *Journal of Spacecraft and Rockets*, Vol. 48, No. 4, 2011, pp. 629–641.

[9] M. Vasile and P. D. Pascale, "Preliminary Design of Multiple Gravity-Assist Trajectories," *Journal of Spacecraft and Rockets*, Vol. 43, No. 4, 2006, pp. 794–805, 10.2514/1.17413.

[10] D. Izzo, V. M. Becerra, D. R. Myatt, S. J. Nasuto, and J. M. Bishop, "Search space pruning and global optimisation of multiple gravity assist spacecraft trajectories," *Journal of Global Optimization*, Vol. 38, June 2007, pp. 283–296.

[11] S. Wagner and B. Wie, "Hybrid Algorithm for Multiple Gravity-Assist and Impulsive Delta-V Maneuvers," *Journal of Guidance, Control, and Dynamics*, Vol. 38, Nov. 2015, pp. 2096–2107, 10.2514/1.G000874.

[12] E. M. Standish, "Keplerian Elements for Approximate Positions of the Major Planets," techreport, JPL/Caltech, N.D.

[13] E. M. Standish and J. G. Williams, "Orbital Ephemerides of the Sun, Moon, and Planets," Unpublished.

[14] A. E. Bryson and Y.-C. Ho, *Applied Optimal Control*. Hemisphere, Washington, 1st ed., 1975.

[15] B. A. Conway, ed., *Spacecraft Trajectory Optimization*. Cambridge, 2010.

[16] R. Storn, "On the Usage of Differential Evolution for Function Optimization," *Proceedings of North American Fuzzy Information Processing*, 1996, pp. 519–523, 10.1109/NAFIPS.1996.534789.

[17] R. Storn and K. Price, "Differential Evolution – A Simple and Efficient Heuristic for global Optimization over Continuous Spaces," *Journal of Global Optimization*, Dec. 1997, p. 341–359.